Easy preparation of small crystalline Pd 2 Sn nanoparticles in solution at room temperature

Vincent Dardun, Tania Pinto, Loïc Benaillon, Laurent Veyre, Jules Galipaud, Clément Camp, V. Meille, Chloé Thieuleux

View Article Online
View Journal

Dalton Transactions

An international journal of inorganic chemistry

Accepted Manuscript

This article can be cited before page numbers have been issued, to do this please use: V. Dardun, T. Pinto, L. Benaillon, L. Veyre, J. Galipaud, C. Camp, V. Meille and C. Thieuleux, *Dalton Trans.*, 2023, DOI: 10.1039/D2DT03476J.

ROYAL SOCIETY OF CHEMISTRY

rsc.li/dalton

View Article Online
DOI: 10.1039/D2DT03476J

ARTICLE

Easy preparation of small crystalline Pd_2Sn nanoparticles in solution at room temperature†

Received 00th January 20xx,
Accepted 00th January 20xx

DOI: 10.1039/x0xx00000x

Vincent Dardun,[a] Tania Pinto,[a] Loïc Benaillon,[a] Laurent Veyre,[a] Jules Galipaud,[b,c] Clément Camp,[a] Valérie Meille,*[d] and Chloé Thieuleux*[a]

We describe here a simple protocol yielding small (<2 nm) crystalline Pd_2Sn nanoparticles (NPs) along with Pd homologues for sake of comparison. These NPs were obtained *via* an organometallic approach using $Pd_2(dba)_3$·dba (dba = dibenzylideneacetone) in THF with 2 equivalents of tributyltin hydride under 4 bars of H_2 at room temperature. The Pd NPs homologues were prepared similarly, using $Pd_2(dba)_3$·dba with 2 equivalents of *n*-octylsilane. These NPs were found crystalline and very small with a similar mean size (ca. 1.5 nm). These NPs were finally used as nanocatalysts in solution for a benchmark Suzuki-Miyaura cross-coupling reaction. The Pd_2Sn NPs were found more active than Pd NPs analogues, exhibiting remarkable performances with Pd loading as low as 13 ppb. This result demonstrates a beneficial effect of tin on palladium in catalysis.

1. Introduction

Metallic nanoparticles (NPs) are central objects in contemporary chemistry and their properties depend on their shape, size and composition. As an example, many chemical reactions are selectively catalyzed by metallic NPs[1] and important efforts are thus currently directed toward the preparation of specific NPs which activity can be correlated to their exposed crystalline phases, the number of facets, edges or corners.[2,3] In this context, the development of specific bimetallic alloyed NPs as for example Pd_xSn_y systems have attracted major attention as the addition of metalloid atoms were found beneficial to enhance the catalytic performances if compared to Pd systems for many reactions such as alcohol[4–8] and formic acid electro-oxidation,[9] oxidation of dihydrogen into hydrogen peroxide,[10] reduction of nitrate[11,12] and nitro-functional groups[13,14] as well as oxygen,[15,16] or hydrogenation of alkynes,[17,18] dienes,[19–22] and heterodienes[23]. However, this is not limited to tin and earth abundant metals could also be used such as Cu[24] or Fe[25] for instance to enhance catalytic performances of catalysts for Heck and Suzuki-Miyaura couplings.

Among the easiest standard routes used to generate Pd_xSn_y bimetallic NPs, one may mention their direct preparation onto supports by chemical[5,13] or thermal[14,23,26] co-reduction of adsorbed Pd(II) and Sn(II) salts or complexes. However, it is extremely difficult to generate well-defined NPs exhibiting controlled size and a unique Pd_xSn_y phase. Alternatively, using classical chemical solution protocols, Pd_xSn_y bimetallic NPs can also be prepared using surfactants or classical stabilizing agents (phosphines and/or amines,[4,9] ammonium salts[10,11] for example) and/or high temperature boiling solvents (oleylamine,[4,6,11] ethylene glycol[7,8] or polyethylene glycol,[21] ionic liquids[18]). Interestingly, monodispersed palladium-tin alloyed NPs with tunable compositions and sizes prepared at high temperature (260 °C) by co-reduction of tin(II) acetate and palladium(II) bromide in the presence of oleylamine and trioctylphosphine were reported and the specific $Pd_{63}Sn_{37}$ NPs exhibited promising catalytic activity in Heck[27] and Suzuki-Miyaura[28] reactions, overpassing those of monometallic Pd NPs. In this context, we investigated the development of Pd_xSn_y NPs using a simple procedure, avoiding the use of surfactant, classical stabilizing agents or high temperature reaction conditions as frequently encountered in the literature. We also avoided the use of metal salts[29] and/or biogenic synthesis[30,31] to avoid the introduction of halides or main group elements (sulfur, phosphorous, nitrogen atoms...) that are not innocent in catalysis and could lead to erroneous conclusions about the effect of tin. We thus developed a synthetic route allowing to generate metallic Pd_2Sn NPs using Bu_3SnH which acts as the tin source to yield the alloyed NPs and ensures the stabilization of the NPs via the presence of surface tributyltin fragments. For sake of comparison, crystalline Pd NPs with similar NPs sizes were also yielded using octylsilane in place of tin as Si atoms will not be incorporated into the NP core and the presence of surface octylsilane fragments will prevent the NPs aggregation.

[a] Université de Lyon, Institut de Chimie de Lyon, Laboratory of Catalysis, Polymerization, Processes & Materials, CP2M UMR 5128 CNRS-UCB Lyon 1-CPE Lyon, CPE Lyon 43 Bd du 11 Novembre 1918, F-69616 Villeurbanne, France. chloe.thieuleux@univ-lyon1.fr
[b] Université de Lyon, Ecole Centrale de Lyon, Laboratory of Tribology and System Dynamics, LTDS UMR CNRS 5513, 36 avenue Guy de Collongues, 69134 Ecully Cedex, France
[c] Université de Lyon, INSA-Lyon, UCBL, MATEIS UMR CNRS 5510, Villeurbanne, France
[d] Université de Lyon, Université Claude Bernard Lyon 1, CNRS, IRCELYON, F-69626, Villeurbanne, France. valerie.meille@ircelyon.univ-lyon1.fr
† Footnotes relating to the title and/or authors should appear here.
Electronic Supplementary Information (ESI) available: [Characterization of the NPs and catalytic study]. See DOI: 10.1039/x0xx00000x

2. Results and discussion

2.1 NPs synthesis

To reach this goal, the Pd_2Sn NPs were obtained by introducing, in a Fischer-Porter reactor, a THF solution of the palladium(0) precursor, namely $Pd_2(dba)_3{\cdot}dba$, and 2 equivalents of tributyltin hydride (Bu_3SnH), acting as the tin source and stabilizing agent. The reactor was further pressurized to 4 bars of H_2 at room temperature overnight, leading to the NPs suspension.

The influence of the number of tin equivalents (1 or 2 equiv.) was studied and 2 equiv. of tributyltin hydride were found to be necessary to yield stable NPs. The use of 1 equivalent of Bu_3SnH led to the rapid decantation of the NPs and extensive formation of aggregates. The optimal preparation thus needs at least 2 equiv. of tin but it is interesting to note that no exogenous stabilizing agent was needed. Note that the resulting NPs were also found extremely stable in solution (up to one year).

We also investigated the role of solvent for such synthetic route and THF was replaced by a non-polar solvent such as toluene, yielding exactly the same bimetallic nanoparticles. The complete conversion of the Pd precursor into particles was monitored by UV-Vis spectroscopy and the characteristic band of the starting Pd complex centered at 530 nm[32] was no longer observed in the resulting colloidal suspension (see Figure 1).

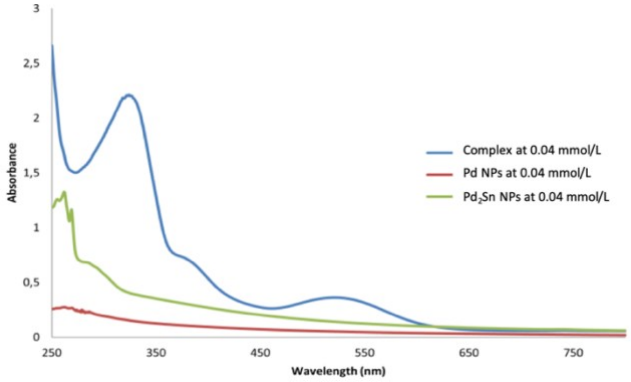

Figure 1 – UV-Visible absorption spectrum of $Pd_2(dba)_3{\cdot}dba$, palladium, and palladium-tin colloids in THF with a Pd concentration of 40 µmol/L at 298 K.

For sake of comparison, we investigated the room temperature preparation of monometallic Pd NPs which exhibit the same features (same NPs size, crystalline Pd(0), absence of hetero-elements such as halides, sulfur, phosphorous or nitrogen atoms). To yield these objects, we used $Pd_2(dba)_3{\cdot}dba$ in toluene and 2 equivalents of *n*-octylsilane in a Fischer-Porter reactor and the resulting solution was stirred under 4 bars of H_2 overnight. Other Pd:Si stoichiometries were investigated here (1 and 1.5 equiv.) yielding very similar Pd NPs exhibiting the same mean size (1.5 nm). *n*-octylsilane was chosen as it is known to stabilize efficiently metallic NPs in solution such as Ru,[33] Pt,[34] Ni[35] and Co[36] without decreasing the catalytic performances of the resulting NPs. It is worth noting that H_2 is not mandatory for such synthesis as *n*-octylsilane is reductive enough to decompose the Pd precursor but the presence of H_2 allows to fasten the reaction kinetics.

2.2 Microscopy analysis

An in-depth characterization of the Pd_2Sn and Pd NPs was performed by HRTEM and STEM-HAADF coupled with EDS. STEM-HAADF micrographs (Figure 2) showed the presence of narrowly distributed and isolated spherical particles with a mean size of 1.5 ± 0.3 nm for both Pd or Pd_2Sn NPs whatever the solvent used (THF or toluene - see ESI for TEM pictures). When EDS analyses were performed onto several single NPs (see ESI – Fig. S5-A), a Pd/Sn ratio of 2 ± 0.3 was found, suggesting the formation of Pd_2Sn. Thus, the excess of tin does not translate into a modification of the NPs composition towards lower Pd/Sn ratios. It is also worth mentioning that neither Sn nor SnO_x nanoparticles were detected by EDS or HRTEM.

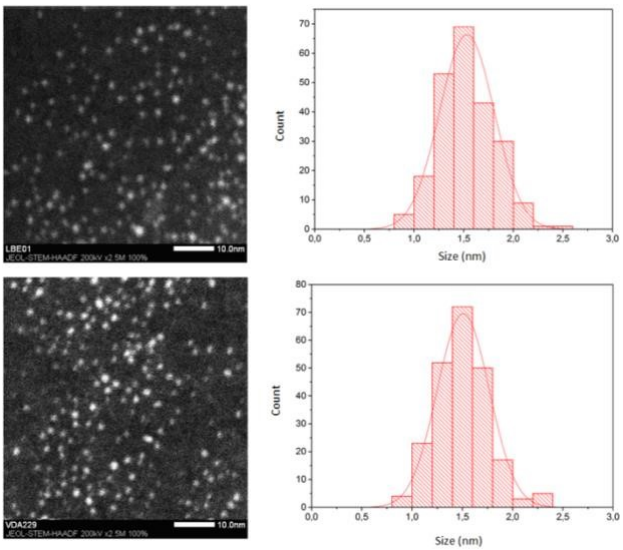

Figure 2 – Size histograms and corresponding STEM-HAADF micrographs of Pd (top) and Pd_2Sn (bottom) nanoparticles (bar scales: 10 nm).

To better understand the crystalline structure of the NPs, HRTEM (Figure 3) was performed on various NPs on which crystallographic arrangements were visible (see ESI – Fig. S6 & S7). It is worth noting that XRD could not provide useful information due to the small NPs size. For both types of NPs, the crystallographic arrangements were observed, and the diffraction patterns obtained by Fourier Transform fitted that of Pd_2Sn in an orthorhombic structure according to JCPDS file n°04-004-2280 (see ESI – Fig. S7) and that of Pd in a hexagonal structure according to JCPDS file n°01-720-0710 (see ESI – Fig S6). The discrepancy between the Pd/Sn ratio introduced experimentally in the reaction and that measured in the particles is not surprising since Pd_2Sn is one of the most thermodynamically stable phase of all the Pd_xSn_y series.[37,38]

View Article Online
DOI: 10.1039/D2DT03476J

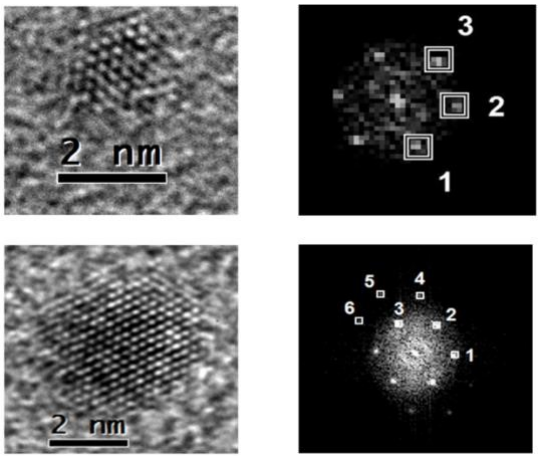

Figure 3 – Representative HRTEM pictures of Pd (top) and Pd_2Sn (bottom) NPs. The arbitrary numbers of the Fourier Transform refer to the vector used for crystallographic indexation (Miller indexes of the reticular plans and angles are shown in ESI-Fig. S6 and S7).

2.3 XPS study

XPS analyses were also used to confirm the oxidation state of both Pd and Sn within the NPs and the influence of Sn onto the oxidation state of Pd. The samples were prepared by wetness impregnation of the Pd_2Sn and Pd NPs colloidal suspensions onto silica supports and further drying under inert conditions. For the Pd NPs, the Pd colloidal suspension was impregnated on SBA-15 that was dehydroxylated at 700°C under high vacuum (10^{-5} mBar), whereas the Pd_2Sn NPs suspension was impregnated onto non-porous silica beads, namely $Degussa_{500}$, dehydroxylated at 500°C under high vacuum (10^{-5} mBar). Note that the samples were introduced into the XPS set-up without exposure to ambient air. Concerning the Pd NPs, the spectrum exhibited a Pd $3d_{5/2}$ signal at 335.7 eV, corresponding to Pd(0)(see ESI-Fig. S8).[39,40] A clear shift in the position of the Pd $3d_{5/2}$ signal was observed for the Pd_2Sn NPs (336.1 eV instead of 335.7 eV) which corresponds to a positive shift of 0.4 eV (Figure 4). Therefore, tin modifies the electron density around palladium, a phenomenon reported on Pd_2Sn nanotubes with a similar positive shift of 0.5 eV.[4] Concerning tin XPS signature, two signals corresponding to the $3d_{5/2}$ and $3d_{3/2}$ orbitals were observed. These asymmetric signals were deconvoluted into one major contribution at 487.1 eV and a minor one at 485.2 eV (Figure 5).[41] The minor contribution was attributed to metallic tin, Sn(0), presumably located at the core of the nanoparticles in the Pd_2Sn alloy. The major contribution was assigned to Sn^{4+} coming from the tributyltin fragments at the surface of the NPs and grafted on the silica surface. Indeed, an excess of tin is needed to yield the bimetallic NPs and during the impregnation of silica with the NPs suspension, such excess of tin precursor could side react with surface silanols leading to $\equiv SiO\text{-}SnBu_3$ surface fragments.

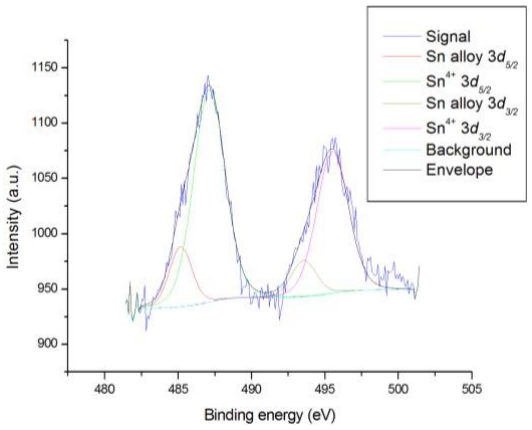

Figure 4 – XPS spectrum and deconvolution of Pd 3*d* core levels of Pd_2Sn colloids impregnated on a $Degussa_{500}$ support.

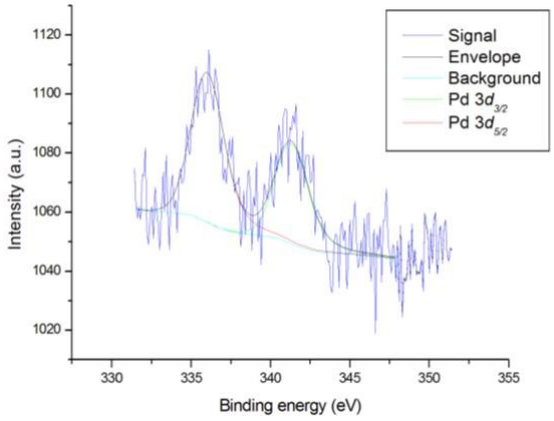

Figure 5 – XPS spectrum and deconvolution of Sn 3*d* core levels of Pd_2Sn colloids impregnated on dehydroxylated silica.

2.4 DRIFTS study

To gather further data about the nature of NPs surface, Diffuse Reflectance Infrared Fourier Transform Spectroscopy (DRIFTS) analyses were performed. The samples were prepared by the addition of an appropriate volume of the colloidal suspension onto dehydroxylated silica[42,43] to reach palladium loadings between 0.5 wt% and 1 wt% and the solvent was further evacuated under vacuum at 135 °C (Figure 6). For Pd NPs, the DRIFT spectrum exhibited the characteristic $\nu_{C\text{-}H}$ stretching vibrations of alkyl groups ($\nu_{Csp^3\text{-}H}$ from 2800 cm^{-1} to 3000 cm^{-1}) suggesting that the Pd NPs are capped by octylsilyl fragments. Some partially hydrogenated forms of dba were also present as demonstrated by $\nu_{Csp^2\text{-}H}$ stretching bands from 3000 cm^{-1} to 3100 cm^{-1}. The Pd_2Sn NPs also exhibited surface alkyl groups as shown by the characteristic $\nu_{Csp^3\text{-}H}$ vibration bands from 2800 cm^{-1} to 3000 cm^{-1}, suggesting that the NPs are capped by tributyltin fragments, while the same $\nu_{Csp^2\text{-}H}$ from the dba were also visible. No Sn-H hydride signal was detected

(expected at 1805-1809 cm^{-1})[44,45] suggesting that the excess of Bu_3SnH was quantitatively evacuated under vacuum.[44]

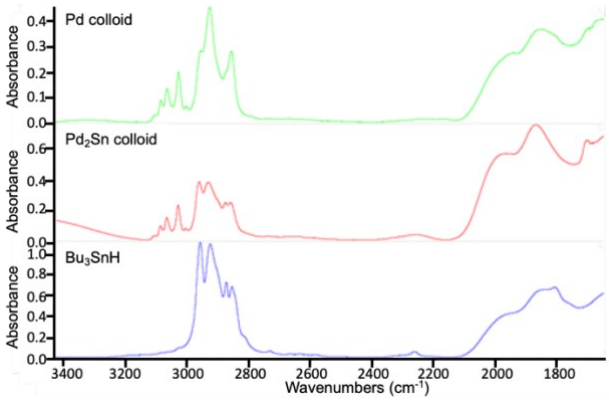

Figure 6 – DRIFTS spectra of the Pd (top) and Pd_2Sn (middle) colloids and Bu_3SnH (bottom) impregnated on dehydroxylated silica.

From these data, and taking into account the only literature precedent describing the preparation of Pt_3Sn NPs in solution using tributyltin hydride as tin precursor to yield Pt-Sn bimetallic NPs,[45] the following mechanism can be suggested for the Pd_2Sn NPs formation: (i) the fast decomposition of $Pd_2(dba)_3{\cdot}dba$ under H_2 leads to low coordinated Pd atoms by partial decoordination and hydrogenation of the dba ligand; (ii) these "naked" Pd atoms then react with the tin precursor, facilitating the alkyl-Sn bond cleavage, hence forming the Pd_2Sn nanoparticles by consumption of both Pd and Sn reagents, leading to a bulk Pd_2Sn phase till all Pd is consumed and decorated by $(alkyl)_xSn$ surface fragments that prevent NPs agglomeration.

2.5 Catalysis

The as-obtained Pd and Pd_2Sn nanoparticles in solution were further tested as catalysts for the Suzuki-Miyaura cross-coupling reaction between 4'-iodoacetophenone (1 equiv.) and phenylboronic acid (1.2 equiv.) in the presence of sodium methoxide (1.5 equiv.) in ethanol at 60 °C under air (see Scheme 1 & Table 1).

The experimental conditions (nature of the base and solvent, number of equivalents of reagents, temperature) were chosen based on a literature precedent which had optimized such parameters.[46] The conversions and yields were determined by GC (see ESI for representative chromatograms) and blank experiments without catalyst were conducted to insure the catalytic performances of these NPs. Importantly, Pd NPs prepared in toluene or THF exhibited the same activity and TON, showing the absence of solvent effect. Preliminary tests were performed using 0.2 mol% of Pd loadings. Both Pd and Pd_2Sn NPs were found highly selective (>99%) towards the cross-coupling product. The catalytic activity of the catalysts was further evaluated as TOF_{50} which was calculated using the slope of the conversion vs. time plots at ca. 50 % conversion to be far from the induction period if any. At 0.2 mol% of Pd loading, the Pd_2Sn NPs exhibited a higher catalytic activity than that of monometallic Pd NPs: TOF_{50} = 22'000 h^{-1} for Pd_2Sn *vs* TOF_{50} = 8'000 h^{-1} for Pd (see ESI, Fig. S11-right). The complete conversion of 4'-iodoacetophenone was reached within 3-5 minutes leading to a TON of 500 (Table 1 - entries 1 & 3). This result highlights the fact that the presence of tin is important to enhance the catalytic activity of Pd.

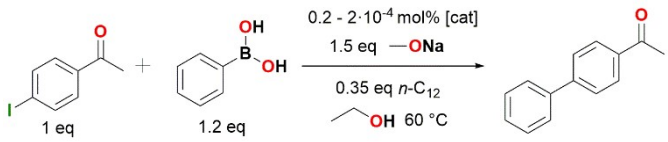

Scheme 1 – Suzuki-Miyaura cross-coupling reaction with 4'-iodoacetophenone and phenylboronic acid in presence of sodium methoxide as base in ethanol.

Further tests were performed using a hundred-fold decrease of the Pd loading (0.002 mol%) and the full conversion of 4'-iodoacetophenone was reached within 4.5 h for Pd NPs (TOF_{50} = 20'000h^{-1}) and 1.5 h for Pd_2Sn NPs (TOF_{50} = 37'000 h^{-1} - see ESI and Fig. S11-left for TOF calculation) with a complete selectivity toward the cross-coupling product (Table 1 - entries 2 & 4). Note that this complete selectivity towards the cross-coupling product is not rare and can be obtained with other standard Pd catalysts. To push further these interesting results, a test at $5{\cdot}10^{-4}$ mol% of Pd loading was conducted with Pd_2Sn NPs, yielding full conversion of 4'-iodoacetophenone within 40 hours (Table 1 - entry 5).

Decreasing further the Pd loading to $2{\cdot}10^{-4}$ mol% led to complete conversion of 4-iodoacetophenone after 3 days with full selectivity towards the cross-coupling product (Table 1 - entry 6) when the test was performed under inert atmosphere. If performed under air as for all the other catalytic tests, no conversion was observed, showing that at such low loading of Pd, air exposure is detrimental for catalysis.

Table 1 – Pd and Pd_2Sn NPs catalytic performances in the Suzuki-Miyaura cross-coupling reaction.

Number	Catalyst	Pd loading (mol%)	Yield (%)	TON	$TOF_{50}(h^{-1})$
1	Pd NPs	$2{\cdot}10^{-1}$	>99	500	8 000
2	Pd NPs	$2{\cdot}10^{-3}$	90	45 000	20 000
3	Pd_2Sn NPs	$2{\cdot}10^{-1}$	>99	500	22 000
4	Pd_2Sn NPs	$2{\cdot}10^{-3}$	>99	50 000	37 000
5	Pd_2Sn NPs	$5{\cdot}10^{-4}$	>99	200 000	25 000
6	Pd_2Sn NPs	$2{\cdot}10^{-4}$	>99	500 000	11 000

Nonetheless, these results highlight that these Pd_2Sn NPs in solution are remarkable catalysts for Suzuki-Miyaura cross-coupling reactions and the performance of Pd_2Sn NPs was found to overpass that of homologous Pd NPs, highlighting the promoting effect of tin.

3. Conclusions

We thus described here simple protocols yielding small, crystalline Pd_2Sn nanoparticles and Pd NPs homologues using an organometallic approach. This specific route allowed yielding the targeted NPs at room temperature without the use

of surfactants, classical stabilizing agents, biogenic conditions or metal salts as to avoid the introduction of halides or main group elements (sulfur, phosphorous, nitrogen atoms...) that might play a role during catalysis.

These Pd and Pd_2Sn NPs were obtained by reaction between $Pd_2(dba)_3$·dba and *n*-octylsilane or tributyltin hydride respectively under 4 bars of H_2 at room temperature overnight. These NPs were further successfully used as catalysts for the Suzuki-Miyaura cross-coupling reaction of 4'-iodoacetophenone and phenylboronic acid. Both Pd and Pd_2Sn were found highly active and selective in the targeted reaction; the performance of Pd_2Sn NPs overpassing that of Pd NPs. Pd_2Sn NPs are indeed promising nanocatalysts for such a benchmark Suzuki-Miyaura cross-coupling reaction, exhibiting very high catalytic performances (TOF = 47'000 h^{-1} and TON = 500'000) with a complete selectivity towards the cross-coupling product, yielding the targeted product with a loading of Pd in solution as low as 13 ppb. These well-defined Pd_2Sn NPs are thus very promising nanocatalysts in solution and could open the way to the development of well-defined heterogeneous catalysts by simple impregnation onto solid supports.

4. Experimental Section

4.1 General considerations

All air-sensitive experiments were conducted under an inert atmosphere using an argon-filled MBRAUN Labmaster 130 glovebox or standard Schlenk line techniques under argon. Glassware was heated in an oven at 90 °C and cooled down under argon atmosphere prior to use. Toluene and THF were distilled from sodium benzophenone ketyl radical, vacuum-transferred to a storage flask and freeze–pump–thaw degassed prior to use and stored under argon in a glovebox. Ethanol was distilled over magnesium, vacuum-transferred to a storage flask and freeze–pump–thaw degassed prior to use and stored under argon in a Strauss flask. All other reagents were acquired from commercial sources (toluene and THF (Sigma-Aldrich), $Pd_2(dba)_3$·dba (Sigma-Aldrich), tributyltin hydride (Sigma-Aldrich), 4'-iodoacetophenone (Sigma-Aldrich), phenylboronic acid (Fluka), sodium methoxide (TCI), n-dodecane (Sigma-Aldrich), ethanol (Carlo Erba) and used as received.

4.2 Synthesis

4.2.1 General procedure for synthesis of Pd NPs in solution. A dry 300 mL Fisher-Porter reaction vessel equipped with a magnetic stirring bar was charged in a glovebox with $Pd_2(dba)_3$·dba (141 mg, 0.25 mmol of Pd), 100 mL of toluene (or THF) and 200 µL of a 1.8 M solution of n-octylsilane in toluene (or THF) (0.37 mmol, 1.5 equiv. compared to Pd). The solution was further degassed to remove argon, put under H_2 (4 bars) atmosphere and stirred at room temperature for 24 h. The reactor was depressurized, and the solution was stored under argon in a Schlenk flask. This resulting brown solution contains 2.45 µmol/mL of palladium and was stored in a fridge at + 4 °C under inert atmosphere.

4.2.2 General procedure for synthesis of Pd_2Sn NPs in solution. A dry 300 mL Fisher-Porter reaction vessel equipped with a magnetic stirring bar was charged in a glovebox with $Pd_2(dba)_3$·dba (86 mg, 0.15 mmol of Pd), 150 mL of toluene or THF and 800 µL of a 0.37 M solution of tributyltin hydride in toluene or THF (0.30 mmol, 2 equiv. compared to Pd). The solution was further degassed to remove argon, put under H_2 (4 bars) atmosphere and stirred at room temperature for 24 h. The reactor was depressurized, and the solution was stored under argon in a Schlenk flask. This resulting brown solution contains 1 µmol/mL of palladium and was stored in a fridge at + 4 °C under inert atmosphere.

4.3 Characterization of the NPs

4.3.1 Transmission Electron Microscopy

Micrographs of palladium and palladium-tin colloids were acquired at the "Centre Technologique des Microstructures", Université Lyon 1, Villeurbanne, France, with a JEOL 2100F transmission electron microscope, using an acceleration voltage of 200 kV under inert conditions using a specific sample holder. The samples were prepared in a glovebox by depositing a drop of colloidal solution on a copper grid covered by a carbon film and let to dry.

4.3.2 UV-Visible spectroscopy

$Pd_2(dba)_3$·dba and palladium NPs were diluted in THF to obtain a range of concentrations of $4{\cdot}10^{-5}$ – $4{\cdot}10^{-4}$ mol/L in terms of Pd concentration and put in a quartz UV-Visible cell equipped with a J. Young valve in a glovebox. UV-Visible studies were performed on a PerkinElmer Lambda 1050 apparatus equipped by Tungsten filament and a D_2 arc lamp with a switch at 319.2 nm. The study was performed in absorbance mode with 1 scan at a speed of 266.25 nm/min. The detector used was a photodemultiplier tube.

4.3.3 DRIFT spectroscopy

Preparation of the samples. The incipient wetness impregnation (IWI) of Pd NPs was carried out under inert conditions (glovebox) by adding the appropriate amount of a colloidal solution (10 times 520 µL of a 8.2 µmol/mL) onto 500 mg of silica SBA-15_{700} (N_2 adsorption/desorption isotherm: V_p: 1.05 cm^3/g, $a_{S,BET}$: 880 m^2/g, $d_{P,BJH,ads}$: 8 nm) to reach palladium loadings in the range of 1 wt%. The wet solid was then stirred at room temperature overnight and finally the solvent was removed overnight *in vacuo* (10^{-5} mbar) at room temperature. For sake of convenience, the IWI of Pd_2Sn was carried out by adding 3 times 265 µL of a 23 µmol/mL onto 250 mg of SBA-15_{700}. The same IWI technique was used for Sn_3BuH using 104 µL of a toluene solution of tin precursor (Bu_3SnH, 2 wt% of Sn) and 100 mg of SBA-15_{700}.

The Diffuse Reflectance Infrared Fourier Transform Spectroscopy (DRIFTS) spectra of the solid samples were collected from a Thermo Scientific Nicolet 6700 FT-IR

spectrometer equipped with an MCT detector. The sample was introduced into the cell under inert atmosphere in a glovebox. The spectral resolution was 2 cm^{-1}, and 64 scans were recorded at 298 K. The reported spectra are presented in an absorbance format.

4.3.4 X-ray photoelectron spectroscopy

Preparation of the samples. A same impregnation method was used for Pd and Pd_2Sn nanoparticles. The Pd colloidal suspension was impregnated on SBA-15_{700} as previously described in the DRIFTS section, whereas the Pd_2Sn NPs suspension was impregnated onto non porous silica beads dehydroxylated at 500°C, namely $Degussa_{500}$ (N_2 adsorption/desorption isotherm: V_p: 1.57 cm^3/g, $a_{S,BET}$: 200 m^2/g, $d_{P,BJH,ads}$: 31 nm) to reach palladium loadings in the range of 0.2 wt%. The wet solids were then stirred at room temperature overnight and finally the solvent was removed overnight *in vacuo* (10^{-5} mbar) at room temperature.

XPS analyses were carried out on a PHI 5000 Versaprobe III apparatus from ULVAC-PHI Inc. A monochromatized Al-K_α source (1486.6 eV) was used with a spot size of 200 µm. A charge neutralization system was used to limit charge effect. The remaining charge effect was corrected fixing the Si 2p peak of SiO_2 from the support material at 103.5 eV. Spectra of Pd and Sn regions were obtained using a pass energy of 27 eV. All the peaks were fitted with CasaXPS software using a Shirley background. Quantification was carried out using the transmission function of the apparatus and angular distribution correction for a 45° angle. Sensitivity factors were extracted from literature[47], they integrate cross section and escape depth correction. The preparation of the sample and their introduction in the XPS set-up were carried out under inert atmosphere.

4.3.5 Gas Chromatography

For GC analysis, a 8890 GC apparatus from Agilent equipped with a HP5 (5% of phenylmethylsiloxane) column was used (30 m length, 320 µm of diameter, 0.25 µm of thickness, and 1.08 min of deadtime). The injected volume was 1 µL with a split ratio of 1:50, in an injection chamber at 250 °C and 12.76 psi. The N_2 vector gas was at 2.9 mL/min at 12.76 psi, corresponding to 46.2 cm/s. Initial oven temperature 70 °C (hold 1 min) and then two ramps were applied: first ramp – 10 °C/min, next temperature 120 °C, second ramp – 40 °C/min, next temperature 300 °C (hold 3 min). The flame ionization detector (FID) was set at 300 °C, with a H_2 flow of 30 mL/min, air flow of 400 mL/min and a make up flow of N_2 of 25 mL/min. Throughout the study, *n*-dodecane was used as GC internal standard to obtain the GC yield for the cross-coupling reaction products.

4.4 Catalytic tests

In an argon filled glovebox, a 50 mL Schlenk flask equipped with a stirring bar was charged with sodium methoxide (82 mg, 1.5 mmol, 1.5 equiv.). Then, using an argon-vacuum line, 4'-iodoacetophenone (246 mg, 1.0 mmol, 1.0 equiv.), phenylboronic acid (146 mg, 1.2 mmol, 1.2 equiv.), *n*-dodecane (80 µL, 0.35 mmol, 0.35 equiv.), and 20 mL of ethanol were introduced before the Pd or Pd_2Sn colloidal catalyst was injected. The reaction mixture was stirred for the indicated time and temperature, before quenching with a mixture of H_2O/EtOAc [2:1] (ca. 0.2 mL per aliquot). The organic layer on top was collected and purified on magnesium sulfate and celite plug before GC analysis.

Author Contributions

V.D., T.P and L.B performed the syntheses and the catalytic tests. L.V. did the microscopy study and the crystallographic resolution. J.G. did the XPS data collection, analysis and deconvolution. V.M. and C.T. curated the data and supervised the work. V.D., L.V., C.C., V.M and C.T. participated to the writing of the article. V.M. and C.T. found the funds and administrated the project.

Conflicts of interest

There are no conflicts to declare.

Acknowledgements

This research was performed in the frame of a French collaborative project funded by the French National Research Agency (ANR) (grant number ANR-18-CE07-0021 (HYPERCAT)) and in the frame of the F.U.I. project "DISCOVER" (F.U.I. standing for "Fonds Unique Interministériel") and we gratefully thank the ANR and the Région Auvergne-Rhône-Alpes, the European Union through the "Fonds Européen de Développement Régional" (FEDER).

Notes and references

1 Z. Xu, H. Yan, Z. Wang, T. Zhang, Y. Ren, T. Fan, Y. Liu and H. Guo, *Mol. Catal.*, 2021, **505**, 111497.

2 O. Margeat, F. Dumestre, C. Amiens, B. Chaudret, P. Lecante and M. Respaud, *Prog. Solid State Chem.*, 2005, **33**, 71–79.

3 L. M. Lacroix, S. Lachaize, A. Falqui, M. Respaud and B. Chaudret, *J. Am. Chem. Soc.*, 2009, **131**, 549–557.

4 Z. Luo, J. Lu, C. Flox, R. Nafria, A. Genç, J. Arbiol, J. Llorca, M. Ibáñez, J. R. Morante and A. Cabot, *J. Mater. Chem. A*, 2016, **4**, 16706–16713.

5 C. Wang, Y. Wu, X. Wang, L. Zou, Z. Zou and H. Yang, *Electrochim. Acta*, 2016, **220**, 628–634.

6 X. Yu, J. Liu, J. Li, Z. Luo, Y. Zuo, C. Xing, J. Llorca, D. Nasiou, J. Arbiol, K. Pan, T. Kleinhanns, Y. Xie and A. Cabot, *Nano Energy*, 2020, **77**, 105116.

7 Z. Cao, X. Liu, X. Meng, L. Cai, J. Chen and P. Guo, *Colloids Surfaces A Physicochem. Eng. Asp.*, 2021, **621**, 126577.

8 C. T. Selepe, S. S. Gwebu, T. Matthews, T. A. Mashola, L. L. Sikeyi, M. Zikhali and N. W. Maxakato, *Nanomaterials*, 2021, **11**, 2725.

9 S. L. A. Bueno, X. Zhan, J. Wolfe, K. Chatterjee and S. E. Skrabalak, *ACS Appl. Mater. Interfaces*, 2021, **13**, 51876–51885.
10 J. Zhang, Q. Shao, Y. Zhang, S. Bai, Y. Feng and X. Huang, *Small*, 2018, **14**, 1703990.
11 Z. Luo, M. Ibáñez, A. M. Antolín, A. Genç, A. Shavel, S. Contreras, F. Medina, J. Arbiol and A. Cabot, *Langmuir*, 2015, **31**, 3952–3957.
12 J. Shi, Y. Gao, L. Zang, Z. Shen and G. Peng, *Environ. Res.*, 2021, **201**, 111577.
13 X. Shan, N. Sui, W. Liu, M. Liu and J. Liu, *J. Mater. Chem. A*, 2019, **7**, 4446–4450.
14 C. L. Daniels, M. Knobeloch, P. Yox, M. A. S. Adamson, Y. Chen, R. W. Dorn, H. Wu, G. Zhou, H. Fan, A. J. Rossini and J. Vela, *Organometallics*, 2020, **39**, 1092–1104.
15 Y. Wu, C. Wang, L. Zou, Q. Huang and H. Yang, *J. Electroanal. Chem.*, 2017, **789**, 167–173.
16 J. Liang, S. Li, Y. Chen, X. Liu, T. Wang, J. Han, S. Jiao, R. Cao and Q. Li, *J. Mater. Chem. A*, 2020, **8**, 15665–15669.
17 E. Esmaeili, A. M. Rashidi, A. A. Khodadadi, Y. Mortazavi and M. Rashidzadeh, *Fuel Process. Technol.*, 2014, **120**, 113–122.
18 C. Dietrich, S. Chen, G. Uzunidis, M. Hähsler, Y. Träutlein and S. Behrens, *ChemistryOpen*, 2021, **10**, 296–304.
19 A. Hammoudeh and S. Mahmoud, *J. Mol. Catal. A Chem.*, 2003, **203**, 231–239.
20 C. Breinlich, J. Haubrich, C. Becker, A. Valcárcel, F. Delbecq and K. Wandelt, *J. Catal.*, 2007, **251**, 123–130.
21 R. Li, Y. Yue, Z. Chen, X. Chen, S. Wang, Z. Jiang, B. Wang, Q. Xu, D. Han and J. Zhao, *Appl. Catal. B Environ.*, 2020, **279**, 119348.
22 E. A. Sales, M. De Jesus Mendes and F. Bozon-Verduraz, *J. Catal.*, 2000, **195**, 96–105.
23 M. Chen, Y. Yan, M. Gebre, C. Ordonez, F. Liu, L. Qi, A. Lamkins, D. Jing, K. Dolge, B. Zhang, P. Heintz, D. P. Shoemaker, B. Wang and W. Huang, *Angew. Chemie Int. Ed.*, 2021, **60**, 18309–18317.
24 D. Zhang, Z. Wei and L. Yu, *Sci. Bull.*, 2017, **62**, 1325–1330.
25 C. Chen, K. Cao, Z. Wei, Q. Zhang and L. Yu, *Mater. Lett.*, 2018, **226**, 63–66.
26 E. A. Sales, J. Jove, M. De Jesus Mendes and F. Bozon-Verduraz, *J. Catal.*, 2000, **195**, 88–95.
27 Y. Li, Y. Dai and X. K. Tian, *Catal. Letters*, 2015, **145**, 1837–1844.
28 Y. Li, T. Wang, B. Yang and X.-K. Tian, *Int. J. Chem. Kinet.*, 2016, **48**, 3–10.
29 S. Swain, M. Bhavya, V. Kandathil, P. Bhol, A. K. Samal and S. A. Patil, *Langmuir*, 2020, **36**, 5208–5218.
30 R. Lakshmipathy, B. Palakshi Reddy, N. C. Sarada, K. Chidambaram and S. Khadeer Pasha, *Appl. Nanosci.*, 2015, **5**, 223–228.
31 S. K. Das, A. Dewan, P. Deka, R. Saikia, S. Thakuria, R. C. Deka, A. J. Thakur and U. Bora, *Curr. Res. Green Sustain. Chem.*, 2022, **5**, 100301.
32 P. D. Harvey, F. Adar and H. B. Gray, *J. Am. Chem. Soc.*, 1989, **111**, 1312–1315.
33 K. Pelzer, B. Laleu, F. Lefebvre, K. Philippot, B. Chaudret, J. P. Candy and J. M. Basset, *Chem. Mater.*, 2004, **16**, 4937–4941.
34 M. Boualleg, J.-M. Basset, J.-P. Candy, P. Delichere, K. Pelzer, L. Veyre and C. Thieuleux, *Chem. Mater.*, 2009, **21**, 775–777.
35 D. Baudouin, K. C. Szeto, P. Laurent, A. De Mallmann, B. Fenet, L. Veyre, U. Rodemerck, C. Copéret and C. Thieuleux, *J. Am. Chem. Soc.*, 2012, **134**, 20624–20627.
36 M. Jakoobi, V. Dardun, L. Veyre, V. Meille, C. Camp and C. Thieuleux, *J. Org. Chem.*, 2020, **85**, 11732–11740.
37 A. F. Lee, C. J. Baddeley, M. S. Tikhov and R. M. Lambert, *Surf. Sci.*, 1997, **373**, 195–209.
38 K. Page, C. S. Schade, J. Zhang, P. J. Chupas, K. W. Chapman, T. Proffen, A. K. Cheetham and R. Seshadri, *Mater. Res. Bull.*, 2007, **42**, 1969–1975.
39 C. Tian, H. Fang, H. Chen, W. Chen, S. Zhou, X. Duan, X. Liu and Y. Yuan, *Nanoscale*, 2020, **12**, 2603–2612.
40 S. Chen, S. Li, R. You, Z. Guo, F. Wang, G. Li, W. Yuan, B. Zhu, Y. Gao, Z. Zhang, H. Yang and Y. Wang, *ACS Catal.*, 2021, **11**, 5666–5677.
41 I. Bondarchuk, F. J. C. S. Aires, G. Mamontov and I. Kurzina, *Crystals*, 2021, **11**, 444.
42 T. Galeandro-Diamant, I. Suleimanov, L. Veyre, M. Bousquié, V. Meille and C. Thieuleux, *Catal. Sci. Technol.*, 2019, **9**, 1555–1558.
43 S. Lassalle, R. Jabbour, P. Schiltz, P. Berruyer, T. K. Todorova, L. Veyre, D. Gajan, A. Lesage, C. Thieuleux and C. Camp, *J. Am. Chem. Soc.*, 2019, **141**, 19321–19335.
44 C. Nédez, A. Theolier, F. Lefebvre, A. Choplin, J. M. Basset and J. F. Joly, *J. Am. Chem. Soc.*, 1993, **115**, 722–729.
45 M. Boualleg, D. Baudouin, J. M. Basset, F. Bayard, J. P. Candy, J. C. Jumas, L. Veyre and C. Thieuleux, *Chem. Commun.*, 2010, **46**, 4722–4724.
46 A. Bourouina, A. Oswald, V. Lido, L. Dong, F. Rataboul, L. Djakovitch, C. de Bellefon and V. Meille, *Catalysts*, 2020, **10**, 989.
47 C. D. Wagner, L. E. Davis, M. V. Zeller, J. A. Taylor, R. H. Raymond and L. H. Gale, *Surf. Interface Anal.*, 1981, **3**, 211–225.